Possible Plasmonic Acceleration of LED Modulationfor Li-Fi Applications

D. V. Guzatov, S. V. Gaponenko & H. V. Demir

Plasmonics

ISSN 1557-1955

Plasmonics
DOI 10.1007/s11468-018-0730-6



Springer

Your article is protected by copyright and all rights are held exclusively by Springer Science+Business Media, LLC, part of Springer Nature. This e-offprint is for personal use only and shall not be self-archived in electronic repositories. If you wish to self-archive your article, please use the accepted manuscript version for posting on your own website. You may further deposit the accepted manuscript version in any repository, provided it is only made publicly available 12 months after official publication or later and provided acknowledgement is given to the original source of publication and a link is inserted to the published article on Springer's website. The link must be accompanied by the following text: "The final publication is available at link.springer.com".



Author's personal copy

Plasmonics
https://doi.org/10.1007/s11468-018-0730-6

Possible Plasmonic Acceleration of LED Modulationfor Li-Fi Applications

D. V. Guzatov[1] · S. V. Gaponenko[2] · H. V. Demir[3,4]

Received: 18 December 2017 / Accepted: 28 February 2018
© Springer Science+Business Media, LLC, part of Springer Nature 2018

Abstract
Emerging LED-based wireless visible light communication (Li-Fi) needs faster LED response to secure desirable modulation rates. Decay rate of an emitter can be enhanced by plasmonics, typically by an expense of efficiency loss because of non-radiative energy transfer. In this paper, metal-enhanced radiative and non-radiative decay rates are shown to be reasonably balanced to get with Ag nanoparticles nearly 100-fold enhancement of the decay rate for a blue LED without loss in overall efficacy. Additionally, gain in intensity occurs for intrinsic quantum yield $Q_0 < 1$. With silver, rate enhancement can be performed through the whole visible. For color-converting phosphors, local field enhancement along with decay rate effects enable 30-fold rate enhancement with gain in efficacy. Since plasmonics always enhances decay rate, it can diminish Auger processes thus extending LED operation currents without efficiency droop. For quantum dot phosphors, plasmonic diminishing of Auger processes will improve photostability.

Keywords Wireless visible light communication · Li-Fi · LED · Plasmonics · Metal-enhanced electroluminescence · Metal-enhanced fluorescence

Introduction

Wireless radiofrequency (RF) communication within restricted rooms and confined areas can possibly be replaced by visible light communication (VLC) based on white LED lighting systems. This concept introduced first in 2000 [1, 2] has nowadays gained an important notion known as light fidelity, "Li-Fi" in short, after well-known Wi-Fi [3]. The Li-Fi paradigm easily breaks RF bandwidth restriction, enables security against tapping from outside the room/area covered by a specific Li-Fi hub, and inhibits undesirable noising and cross-talk issues, and therefore not only can be readily integrated in residential communication services but also in special interference-sensitive areas like hospitals or aircrafts [4]. To make efficient use of white LEDs in Li-Fi networks, all possible ways of high-speed modulation should be examined. A typical commercial white LED consists of a blue LED (the most common case is $\lambda_{max} = 450$ nm emission wavelength maximum) and phosphors converting a portion of blue light into green and red radiation. Therefore, in case that the whole visible is expected to carry on optical data, both blue LED electron-hole pair recombination rate and phosphor active component decay rate may become the critical parameters defining the data processing rate limit. If the phosphor emission is filtered at the receiver end, then only the blue electroluminescence matters for high-speed optical modulation.

It is reasonable to evaluate all possible options for plasmonic acceleration of decay rate for both LED and phosphor in the context of high-speed Li-Fi sources. Plasmonic enhancement is well established for photoluminescence (PL) [5–12]. PL intensity enhancement is defined by interplay of local incident field enhancement and radiative and non-radiative decay rates enhancement promoted by proximity of a metal nanobody. Efficient 10^3-fold acceleration of photoluminescence decay without essential loss in quantum yield has been recently experimentally demonstrated with silver cubical particles [12]. Recently, a number of groups have reported on LED intensity

✉ S. V. Gaponenko
s.gaponenko@ifanbel.bas–net.by

[1] Yanka Kupala State University of Grodno, 230023 Grodno, Belarus

[2] B. I. Stepanov Institute of Physics, National Academy of Sciences, 220072 Minsk, Belarus

[3] Department of Electrical and Electronics Engineering, Department of Physics, and UNAM–Institute of Materials Science and Nanotechnology, Bilkent University, 06800 Ankara, Turkey

[4] LUMINOUS! Center of Excellence for Semiconductor Lighting and Displays, School of Electrical and Electronic Engineering, School of Physical and Mathematical Sciences, Nanyang Technological University, 50 Nanyang Ave, Singapore 639798, Singapore

Published online: 07 March 2018

Author's personal copy

enhancement using plasmonic resonances of Ag and Au nanoparticles (NPs) including both quantum well-based LEDs [12, 13] and colloidal quantum dot-based LEDs [14–16], the latter being of special interest in the context of the colloidal nanophotonics platform [17–19] since metal colloidal NPs can be integrated therein. Enhancement of radiative and non-radiative decay rates promoted by metal nanoparticles means that modulation rate of data transfer systems can be accelerated accordingly. It is important to look for favorable balance of radiative versus non-radiative process enhancement to enable modulation rate speedup without undesirable noticeable loss in overall efficiency since dominating enhancement of non-radiative process will result in fall of the intrinsic emission quantum yield Q. The above tasks are examined in the present paper.

Results and Discussion

We examine plasmonic effects on decay rates based on the model of light emission by a dipole near a metal spherical NP. The model accounts for the scattering that has been shown [10] to be crucial for NPs bigger than 20 nm, which is the case for the typical experimental situations. It was shown to provide reasonable explanation for the abovementioned experimental implementations [13–15] of LED intensity enhancement [16]. Here, the multi-parametric problem is examined including the material type (Au and Ag), NP size, metal-emitter spacing, emission wavelength, and intrinsic quantum yield. The results obtained show that plasmonic enhancement of decay rates both for blue LED and color-converting phosphors in white LEDs as well as for green and red LEDs in case of making LED clusters for white light generation is feasible without noticeable loss in overall efficiency or even along with its increase.

We use the model [10] based on a modified radiative decay rate of a dipole emitter near a metal nanobody by means of computing its modified dipole transitions probability. The most favorable case is considered of a dipole moment oriented along the line connecting an emitter with the NP center. Change in the total decay rate $\gamma = \gamma_0 + \gamma_{\text{int}}$ breaks into plasmonic effect on radiative and non-radiative processes,

$$\frac{\gamma^*}{\gamma} = \frac{\gamma_r + \gamma_{\text{nr}}}{\gamma_0 + \gamma_{\text{int}}} = Q_0 \frac{\gamma_r + \gamma_{\text{nr}}}{\gamma_0}, \quad Q_0 = \frac{\gamma_0}{\gamma_0 + \gamma_{\text{int}}} \tag{1}$$

where γ^* is the modified total decay rate in the presence of a nanobody, γ_0 is the intrinsic radiative spontaneous decay rate, γ_{int} is the intrinsic non-radiative decay rate describing internal losses of an emitter, γ_r and γ_{nr} are the radiative and non-radiative decay rates of an emitter in the presence of a metal nanobody, respectively, and Q_0 is the intrinsic quantum yield of the emitter. For the dipole orientation chosen, the required values read [6, 10, 20].

$$\frac{\gamma_r}{\gamma_0} = \frac{3}{2} \sum_{p=1}^{\infty} p(p+1)(2p+1) \left| \frac{\psi_p(k_0 r_0 n)}{(k_0 r_0 n)^2} + A_p \frac{\zeta_p(k_0 r_0 n)}{(k_0 r_0 n)^2} \right|^2, \tag{2}$$

$$\frac{\gamma_r + \gamma_{nr}}{\gamma_0} = 1 + \frac{3}{2} \sum_{p=1}^{\infty} p(p+1)(2p+1) \text{Re} \left\{ A_p \left(\frac{\zeta_p(k_0 r_0 n)}{(k_0 r_0 n)^2} \right)^2 \right\}, \tag{3}$$

where $\psi_p(x) = \text{xj}_p(x)$ and $\zeta_p(x) = \text{xh}_p^{(1)}(x)$ are Ricatti–Bessel functions, $r_0 = a + \Delta r$ is the distance for a NP center to an emitter, k_0 is the wave number in vacuum, n is the medium refractive index, and $j_p(x)$ and $h_p^{(1)}(x)$ are the spherical Bessel functions, and

$$A_p = -\left(\frac{\sqrt{\varepsilon}\psi_p(k_0 a\sqrt{\varepsilon})\psi_p'(k_0 an) - n\psi_p'(k_0 a\sqrt{\varepsilon})\psi_p(k_0 an)}{\sqrt{\varepsilon}\psi_p(k_0 a\sqrt{\varepsilon})\zeta_p'(k_0 an) - n\psi_p'(k_0 a\sqrt{\varepsilon})\zeta_p(k_0 an)} \right)$$

is one of the Mie coefficients for the field reflected from a NP surface, primes denote derivatives, a is NP radius, and ε is the metal complex dielectric permittivity. When an emitter is moved far from the metal NP, i.e., when $\Delta r \to \infty$ holds, one has $\gamma_r/\gamma_0 \to 1$ and $(\gamma_r + \gamma_{\text{nr}})/\gamma_0 \to 1$.

Calculations were made for 20–100 nm Ag and Au NPs with $\varepsilon(\lambda)$ function according to ref. 21 with $n = 1.5$ which is typical for polymers. Notably, Eqs. (1)—(3) show that plasmonic effect on total decay rate does not depend on the absolute values of intrinsic radiative γ_0 and non-radiative γ_{int} decay rates, i.e., it is independent of intrinsic emitter lifetime. Acceleration factor of the total decay rate is entirely defined by Q_0, emission spectrum, metal dielectric permittivity, nanoparticle size, and emitter-metal spacing.

Acceleration in radiative decay component (Fig. 1) features pronounced size dependence from so-called morphological resonance arising from light scattering for sizes higher than 20 nm. These size-dependent enhancement spectra remarkably correlate with size-dependent nanoparticles extinction spectra (Fig. 2).

Enhancement for non-radiative component (Fig. 3) also features size dependence but it exhibits steep decrease with wavelength and distance. For wavelengths > 440 nm, it vanishes at spacing > 15 nm whereas enhancement of radiative decay measures up to 10–15 at the same conditions. This difference in radiative and non-radiative rate behavior allows for efficient enhancement of the total decay rate without noticeable loss in efficiency. Therefore, for every emitter independent of intrinsic quantum yield Q_0, modulation rate at these conditions will rise without efficiency loss since quantum yield will not fall down. For $Q_0 < 1$, non-radiative decay enhancement may become not very valuable for efficiency since it will be added to the existing intrinsic non-radiative rate, and then even higher acceleration of modulation rate can be expected using closer position of the emitter to the

Author's personal copy

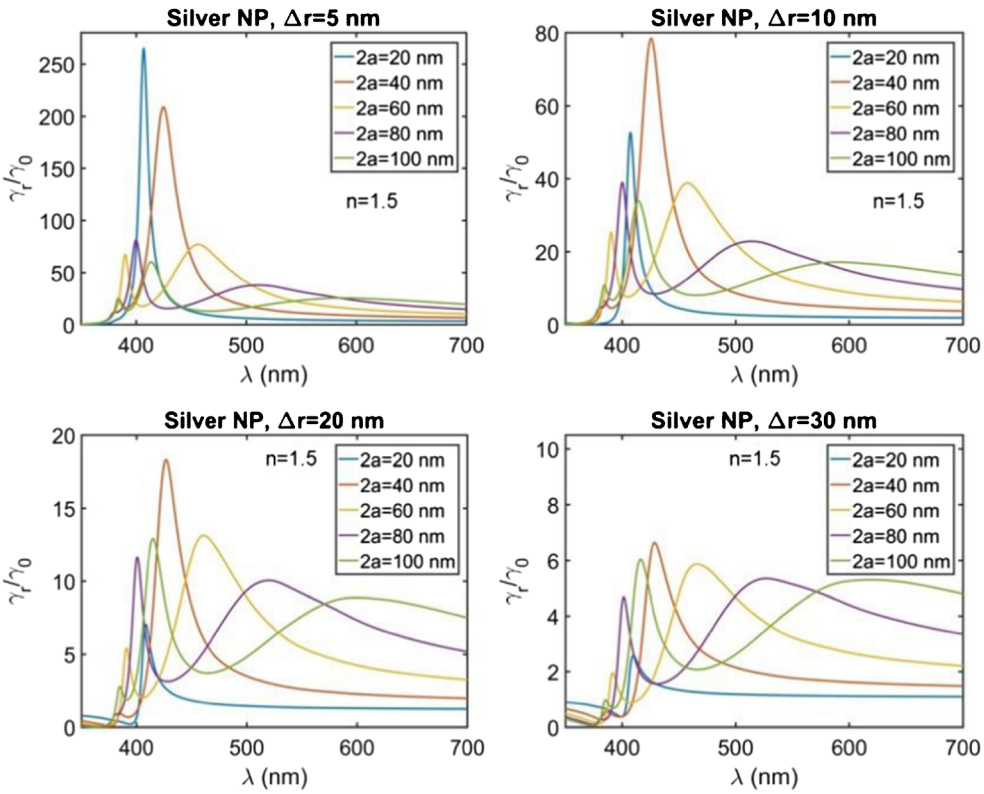


Fig. 1 Calculated modified radiative decay rate for an emitter near an Ag nanoparticle with diameters 20, 40, 60, 80, and 80 nm and spacings 5, 10, 20, and 30 nm

metal, e.g., if we consider $Q_0 = 0.5$, then for 450-nm wavelength, 60-nm NP diameter and 5-nm distance, one has total decay rate enhancement about 100 times and quantum yield rises up from 0.5 to 0.7. Thus, for this example chosen, not only modulation rate will speed up but intensity will rise as well.

Figures 1, 3, and 4 show that enhancement is also possible for green, yellow, and red LEDs that can be used in case of designing white LED as a cluster consisting of three to four discrete LEDs to get options for desirable emission spectrum depending on a consumer's demand.

For more commonly used white LEDs based on a blue LED together with a color-converting phosphor, metal effect on phosphor photoluminescence should be examined.

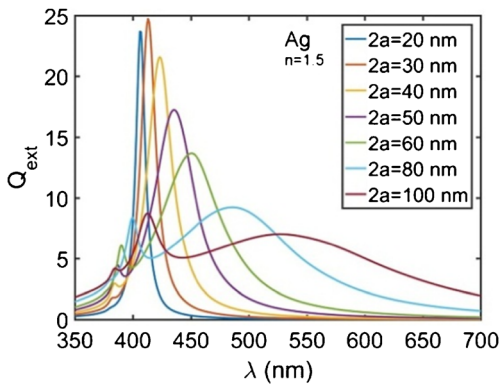


Fig. 2 Calculated extinction spectral of Ag nanoparticles

Enhancement for the total decay rate is feasible for the phosphor spectrum (500–650 nm) by a factor of 20–30 mainly owing to radiative component enhancement, i.e., without overall intensity loss. Additionally, one should bear in mind that for phosphors optical excitation is the case. Therefore, the overall photoluminescence intensity I_0 rises to I owing to the blue LED incident local field **E** enhancement [10] in accordance with

$$\frac{I}{I_0} = \frac{|\mathbf{E}|^2}{|\mathbf{E}_0|^2} \frac{\gamma_r}{\gamma_r + \gamma_{nr}}. \tag{4}$$

Figure 5 presents intensity enhancement maps for phosphor excitation by a blue LED. One can see 50-nm silver NPs enable more than 60-fold increase in intensity over the whole phosphor spectrum. This allows for higher overall rate enhancement factors by using closer distance where nonradiative transition rates rise considerably or even dominate over radiative rate. Based on data presented in Figs. 4 and 5, 30 to 40 rate enhancement factors can be foreseen for phosphor in white LEDs without loss in efficacy or even with simultaneous efficiency enhancement. It is noteworthy that superior photoluminescence enhancement excited at 450 nm inherent for 50- and 60-nm particles remarkably correlates with their extinction maxima very close to the above excitation wavelength (see Fig. 2). Higher enhancement factors can be foreseen for elongated NPs that can be developed by

Author's personal copy

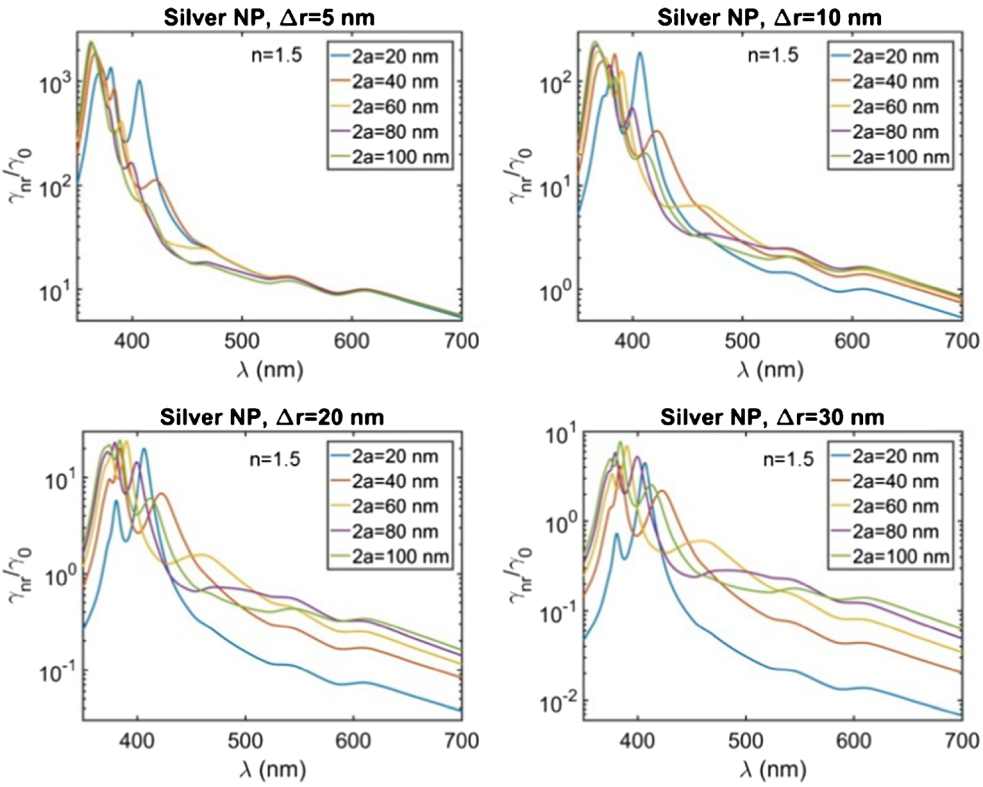


Fig. 3 The same as in Fig. 1 but for modified non-radiative decay rate

means of colloidal techniques [22]. Shaping silver NPs beyond spherical ones will result in morphological resonances where radiative decay enhancement overtakes non-radiative one [12, 23, 24]. However, at the same time, radiative rate enhancement spectrum may shift considerably towards longer wavelengths thus making operation in the blue impossible.

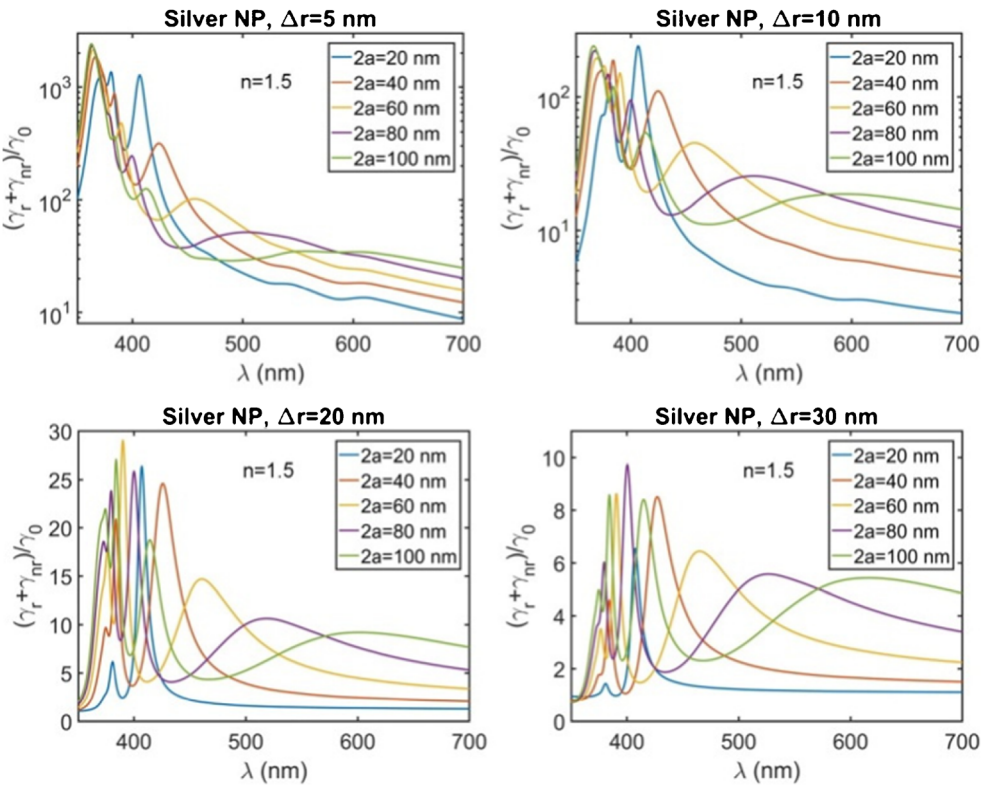


Fig. 4 The same as in Fig. 1 but for the full decay rate

Author's personal copy

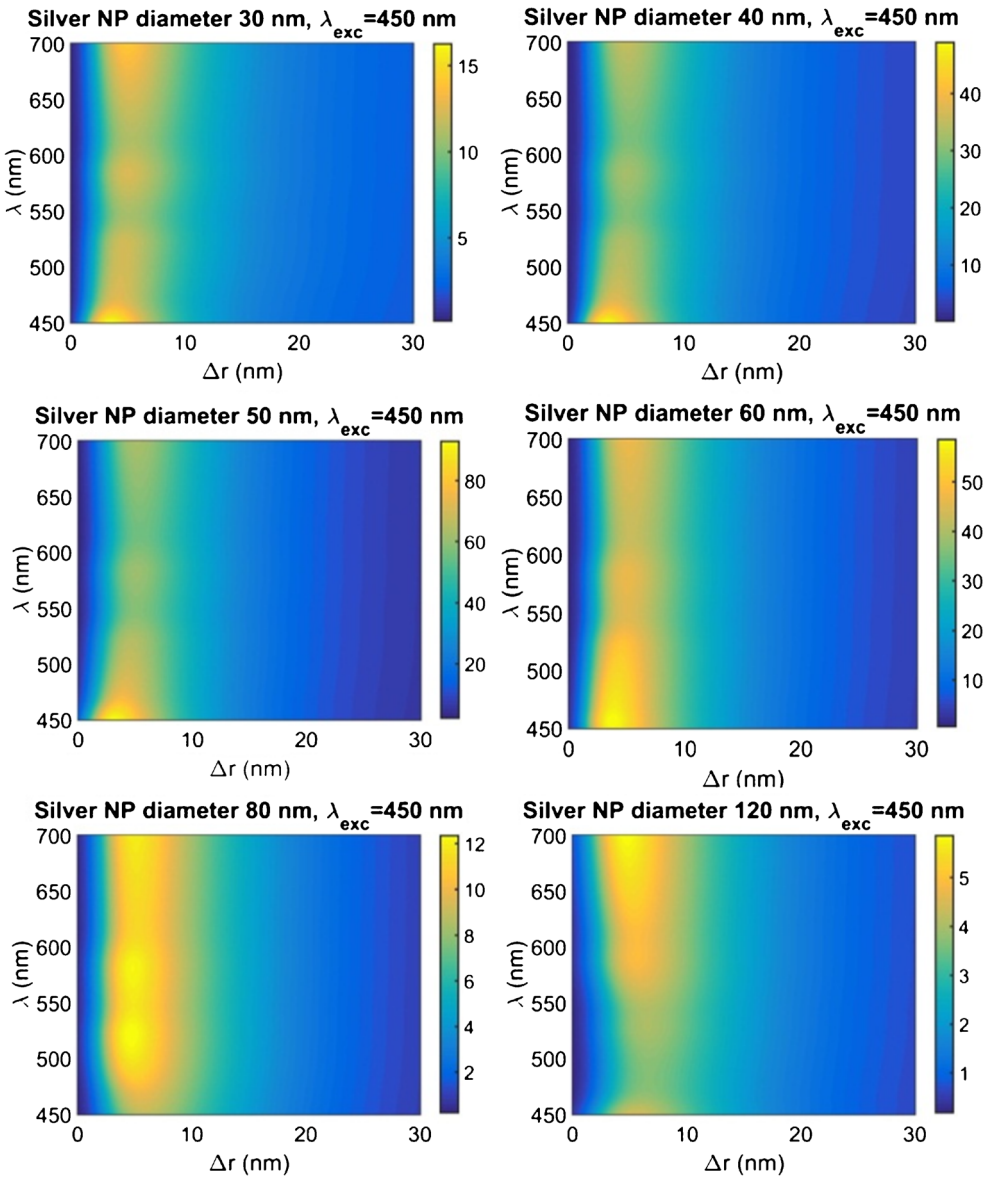


Fig. 5 Enhancement factor for intensity of a phosphor photoluminescence near an Ag nanoparticle with diameters 30 to 120 nm as function of emission wavelength and spacing; excitation wavelength is 450 nm. Intrinsic quantum yield $Q_0 = 1$, and ambient medium refractive index $n_m = 1.5$

Gold NPs are found to be much less efficient in Li-Fi applications (Fig. 6). First, blue LED rate enhancement is not possible at all. Only green and red emitters can be affected by gold NPs, and color-converting phosphor rate in white LEDs can also be affected. Second, acceleration strongly changes across green-red spectrum (550–650 nm). Third, in most cases, non-radiative decay dominates and thus modulation acceleration will occur at the expense of losses in quantum yield. For these reasons, only a few representative graphs are plotted for Au NPs in Fig. 6; 550-nm enhancement of non-radiative decay dominates and will cause undesirable efficiency loss. For 600 nm, 40-fold total decay rate enhancement is possible with equally enhanced radiative and non-radiative decays. That means, for $Q_0 = 1$, quantum yield will drop to 0.5 but for $Q_0 < 1$ the quantum yield will not change. For 650 nm, nearly 30-fold enhancement of the total decay rate is possible without considerable loss in the quantum efficiency. One can see that actually only in the red Au NPs offer rate enhancement without considerable drop of quantum efficacy. It is noteworthy that, unlike silver, shaping of gold nanoparticles is not efficient for the visible since morphological resonance(s) will shift outside the visible to the infrared. Further progress can be foreseen with integrated nanoantenna components [25–28].

It is important that since plasmonics always enhances decay rate, it can principally diminish the role of Auger processes in every semiconductor light-emitting device. Auger recombination at higher electron-hole pair density is considered as the most probable reason for the known efficiency droop in InGaN commercial LEDs at higher currents [29]. Plasmonic enhancement of recombination rate will create a “bypass” for

Author's personal copy

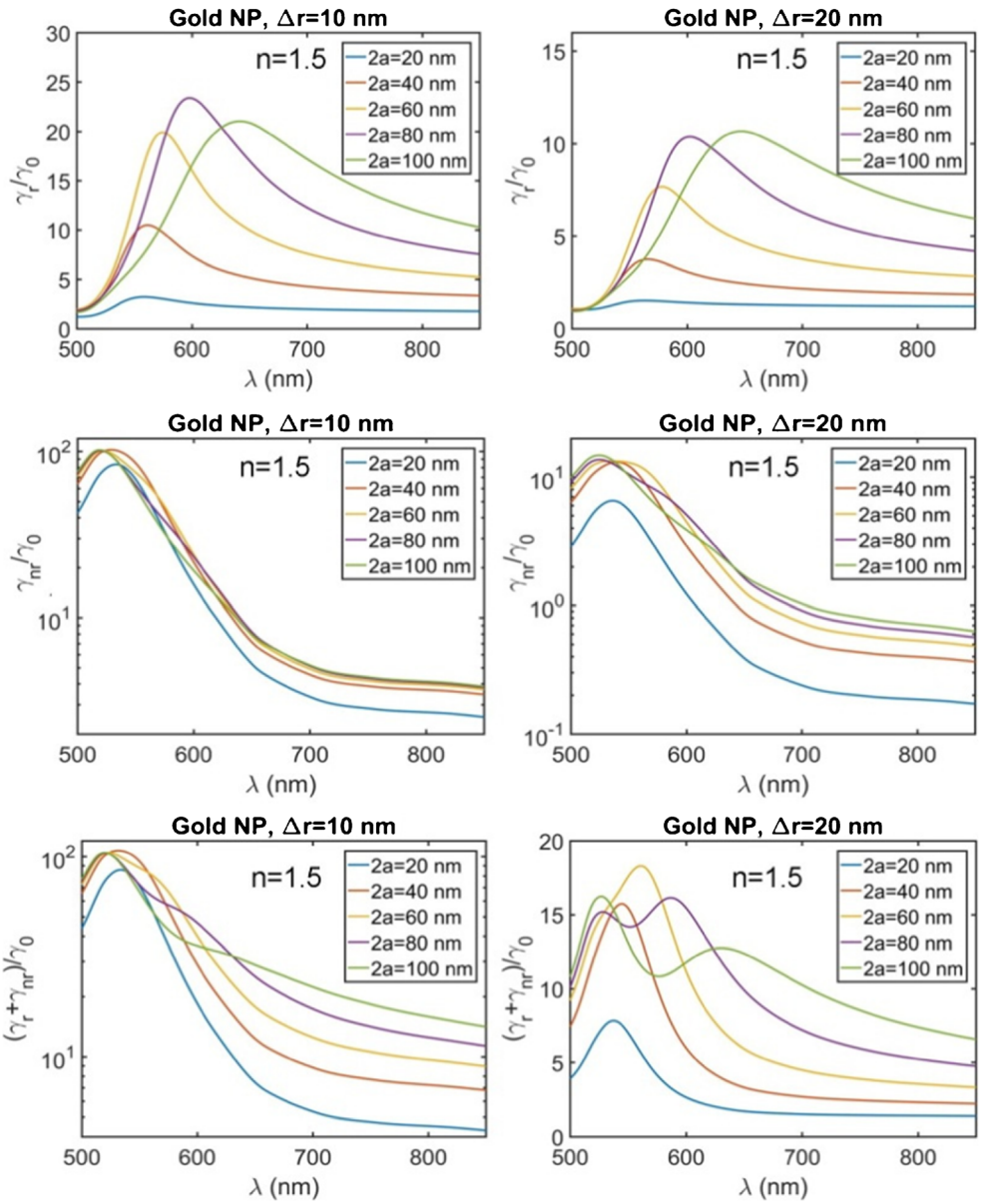


Fig. 6 (Top) Radiative, (middle) non-radiative, and (bottom) total decay rate modification for Au nanoparticles at (left) 10- and (right) 20-nm spacing. Ambient medium refractive index $n = 1.5$

all other photoinduced processes including Auger recombination. The latter is known also to deteriorate colloidal quantum dot photostability. In the context of recent emergence of colloidal quantum dot LEDs [30], the Auger issue may become a critical obstacle towards their commercial applications since Auger recombination is known as the principal reason of luminescence degradation for colloidal nanocrystals [31]. For photoluminescent colloidal quantum dots, very thick or gradient shell has been successfully applied to diminish Auger recombination [32–34]. A thick shell inhibits undesirable photoionization favored by Auger processes whereas a gradient shell inhibits Auger process itself owing to minimized wave functions overlap of higher and lower electron states. However, complicated core-shell design may have negative impact on electron and hole injection efficiency in colloidal LEDs and can become inappropriate in every electroluminescent device. Here, plasmonics may become a reasonable way to inhibit Auger processes while keeping carrier injection conditions unperturbed. For color-converting quantum dot phosphors, along with gain in intensity, plasmonic effects will definitely improve photostability by diminishing Auger processes.

Conclusions

In conclusion, we predict considerable acceleration of blue LED decay rate up to 100 times using silver nanoparticles without essential loss in efficacy. Green and yellow emission rates can be enhanced by a factor of 20–30 with loss in

Author's personal copy

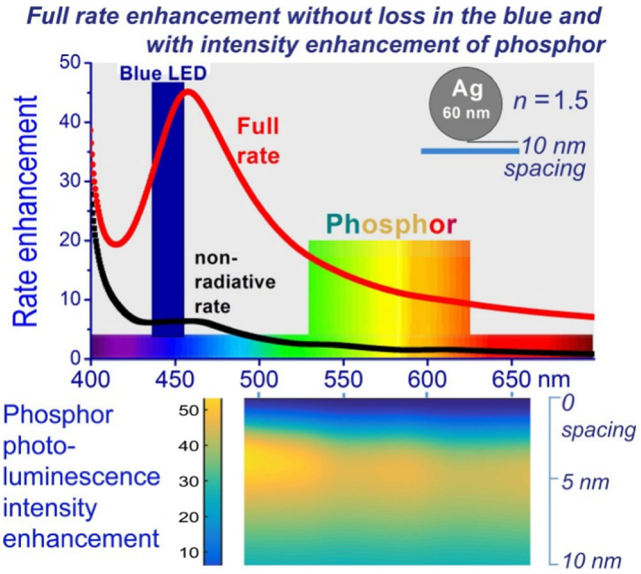


Fig. 7 A brief summary of the LED performance enhancement by metal nanoparticles (silver, 60 nm diameter). The full rate can be enhanced both for electroluminescence in the blue (LED range) and for photoluminescence in the phosphor range whereas the non-radiative decay does not change dramatically. At the same time, phosphor emission intensity can be enhanced as well depending on metal-phosphor spacing (shown in the bottom)

efficiency which can be compensated in the case of an optically pumped phosphor within a white LED by local incident field enhancement. Red emission rate can be enhanced both with silver and gold nanoparticles by a factor of 30–40. Silver nanoparticles are found to be useful within the whole visible whereas gold ones are efficient mainly in the red. A representative sketch of the overall metal-enhanced white LED performance is given in Fig. 7 for one particular case (60-nm diameter silver nanospheres). These findings indicate the prospect for the essential improvement of white LED performance in the context of data transfer rate in Li-Fi setup. Additionally, since plasmonics always enhances decay rate, it can principally diminish the role of Auger processes in semiconductor light-emitting devices thus extending operation currents and inhibiting the droop in efficiency, both for quantum well- and quantum dot-based LEDs. For color-converting quantum dot phosphors in white LEDs, plasmonics is expected to increase photostability owing to bypassed Auger recombination.

Funding The work has been supported by BRFFR-TUBITAK no. F16T/A-010 and TUBITAK no. 115E679, and in part by Singapore National Research Foundation under NRF-NRFI2016-08.

References

1. Tanaka Y, Haruyama S, Nakagawa M (2000) Wireless optical transmissions with the white colored LED for the wireless home links. In: Proc of the 11th Int Symp Personal, Indoor and Mobile Radio Communications (London), p 1325–1328
2. Komine T, Nakagawa M (2004) Fundamental analysis for visible-light communication system using LED lights. IEEE Trans Consum Electron 50:100–107
3. Dimitrov S, Haas H (2015) Principles of LED light communications: towards networked Li-Fi. Cambridge University Press, Cambridge
4. Tsonev D, Videv S, Haas H (2014) Light fidelity (Li-Fi): towards all-optical networking. Proc SPIE 9007: 900702-1-10
5. Geddes CD (ed) (2010) Metal-enhanced fluorescence. Wiley-VHC, Weinheim
6. Klimov VV (2009) Nanoplasmonics. Fizmatlit, Moscow
7. Gaponenko SV (2010) Introduction to nanophotonics. Cambridge University Press, Cambridge
8. Törmä P, Barnes WL (2015) Strong coupling between surface plasmon polaritons and emitters. Rep Progr Phys 78:013901
9. Klimov VV, Guzatov DV (2007) Optical properties of an atom in the presence of a two-nanosphere cluster. Quant Electron 37:209–216
10. Guzatov DV, Vaschenko SV, Stankevich VV, Lunevich AY, Glukhov YF, Gaponenko SV (2012) Plasmonic enhancement of molecular fluorescence near silver nanoparticles: theory, modeling, and experiment. J Phys Chem C 116:10723–10733
11. Gaponenko SV (2014) Satyendra Nath Bose and nanophotonics. J Nanophotonics 8:087599
12. Akselrod GM, Weidman MC, Li Y, Argyropoulos C, Tisdale WA, Mikkelsen MH (2016) Efficient nanosecond photoluminescence from infrared PbS quantum dots coupled to plasmonic nanoantennas. ACS Photonics 3:1741–1746
13. Cho C-Y, Lee S-J, Song J-H, Hong S-H, Lee S-M, Cho Y-H, Park S-J (2011) Enhanced optical output power of green light-emitting diodes by surface plasmon of gold nanoparticles. Appl Phys Lett 98:051106
14. Gu X, Qiu T, Zhang W, Chu PK (2011) Light-emitting diodes enhanced by localized surface plasmon resonance. Nanoscale Res Lett 6:199–210
15. Yang X, Hernandez-Martinez PL, Dang C, Mutlugun E, Zhang K, Demir HV, Sun XW (2015) Electroluminescence efficiency enhancement in quantum dot light-emitting diodes by embedding a silver nanoisland layer. Adv Opt Mater 3:1439–1445
16. Kim NY, Hong SH, Kang JW, Myoung N, Yim SY, Jung S, Lee K, Tu CW, Park SJ (2015) Localized surface plasmon-enhanced green quantum dot light-emitting diodes using gold nanoparticles. RSC Adv 5:19624–19629
17. Pan J, Chen J, Zhao D, Huang Q, Khan Q, Liu X, Tao Z, Zhang Z, Lei W (2016) Surface plasmon-enhanced quantum dot light emitting diodes by incorporating gold nanoparticles. Opt Exp 24:A33–A39
18. Gaponenko SV, Demir HV, Seassal C, Woggon U (2016) Colloidal nanophotonics: the emerging technology platform. Opt Expr 24: A430–A433
19. Erdem T, Demir HV (2011) Semiconductor nanocrystals as rare-earth alternatives. Nature Phot 5:126–129
20. Klimov VV, Letokhov VS (2005) Electric and magnetic dipole transitions of an atom in the presence of spherical dielectric interface. Laser Phys 15:61–73
21. Johnson PB, Christy RW (1972) Optical constants of the noble metals. Phys Rev B 6:4370–4379
22. Sau TK, Rogach AL (eds) (2012) Complex-shaped metal nanoparticles: bottom-up syntheses and applications. John Wiley & Sons, Hoboken
23. Gandra N, Portz C, Tian L, Tang R, Xu B, Achilefu S, Singamaneni S (2014) Probing distance-dependent plasmon-enhanced near-infrared fluorescence using polyelectrolyte multilayers as dielectric spacers. Angew Chem Int Ed 53:866–870

Author's personal copy

24. Lu G, Zhang T, Li W, Hou L, Liu J, Gong Q (2011) Single-molecule spontaneous emission in the vicinity of an individual gold nanorod. J Phys Chem C 115:15822–15832
25. Mühlschlegel P, Eisler HJ, Martin OJF, Hecht B, Pohl DW (2005) Resonant optical antennas. Science 308:1607–1609
26. Rogobete L, Kaminski F, Agio M, Sandoghdar V (2007) Design of plasmonic nanoantennae for enhancing spontaneous emission. Opt Lett 32:1623–1625
27. Dregely D, Taubert R, Dorfmüller J, Vogelgesang R, Kern K, Giessen H (2011) 3D optical Yagi-Uda nanoantenna array. Nat Commun 2:267–270
28. Tsakmakidis KL, Boyd RW, Yablonovitch E, Zhang X (2016) Large spontaneous-emission enhancements in metallic nanostructures: towards LEDs faster than lasers. Opt Exp 24:17916–17927
29. Iveland J, Martinelli L, Peretti J, Speck JS, Weisbuch C (2013) Direct measurement of Auger electrons emitted from a semiconductor light-emitting diode under electrical injection: identification of the dominant mechanism for efficiency droop. Phys Rev Lett 110:177406
30. Su L, Zhang X, Zhang Y, Rogach AL (2016) Recent progress in quantum dot based white light-emitting devices. Top Curr Chem 374:1–25
31. Gaponenko SV (1998) Optical properties of semiconductor nanocrystals. Cambridge Uni Press, Cambridge
32. Bae WK, Kwak J, Park JW, Char K, Lee C, Lee S (2009) Highly efficient green-light-emitting diodes based on CdSe@ ZnS quantum dots with a chemical-composition gradient. Adv Mat 21:1690–1694
33. Chen Y, Vela J, Htoon H, Casson JL, Werder DJ, Bussian DA, Klimov VI, Hollingsworth JA (2008) "Giant" multishell CdSe nanocrystal quantum dots with suppressed blinking. J Am Chem Soc 130:5026–5027
34. Cragg GE, Efros AL (2010) Suppression of Auger processes in confined structures. Nano Lett 10:313–317